International Journal of Electrical, Electronic and Communication Sciences
ISSN: 2517-9438
Vol:6, No:10, 2012

MIMO Performances in Tunnel Environment: Interpretation from the Channel Characteristics

C. Sanchis-Borras, J. M. Molina-Garcia-Pardo, P. Degauque, and M. Lienard

***Abstract*—**The objective of this contribution is to study the performances in terms of bit error rate, of space-time code algorithms applied to MIMO communication in tunnels. Indeed, the channel characteristics in a tunnel are quite different than those of urban or indoor environment, due to the guiding effect of the tunnel. Therefore, MIMO channel matrices have been measured in a straight tunnel, in a frequency band around 3GHz. Correlation between array elements and properties of the MIMO matrices are first studied as a function of the distance between the transmitter and the receiver. Then, owing to a software tool simulating the link, predicted values of bit error rate are given for VLAST, OSTBC and QSTBC algorithms applied to a MIMO configuration with 2 or 4 array elements. Results are interpreted from the analysis of the channel properties.

***Keywords*—**MIMO, propagation channel, space-time algorithms, tunnel.

I. Introduction

THE increase of the communication performances in a tunnel environment is a challenging problem. One important application deals with train-to-track communications which often need a high bit rate and reliable link. To improve the performances of this link, Multiple-Input Multiple-Output (MIMO) is a well-known technique and for urban, suburban and indoor environments a large number of papers have already been published [1], [2]. However, the propagation characteristics in a tunnel are quite different since only rays impinging the tunnel walls with a grazing angle of incidence do not suffer a too strong attenuation and contribute to the total field. The spread of the angle of arrival or of departure of the rays are small and one can thus wonder if MIMO techniques still give interesting results. Theoretical and experimental works undertaken these last years have shown that the channel capacity is nevertheless improved by using MIMO techniques, compared to the Single-Input Single-Output (SISO) case [3], [4]. The better results are obtained if the transmitting (Tx) and receiving (Rx) array elements are aligned perpendicularly to the tunnel axis [3]. This can be explained by the concept of modal diversity as described in [5], [6].

However, to clearly point out the interest of using MIMO in tunnels, the comparison with SISO system must also be done on the bit error rate. In a preliminary approach [7], it was shown that, for a given length of the antenna array, polarization diversity does not present a major interest, the waves remaining polarized. In this paper, we will thus only consider co-polarized vertical antennas. We extend the work in [7] first by considering MIMO (2,2) and MIMO (4,4) configurations, i.e., with 2 or 4 array elements, and by using Orthogonal Space-Time Block codes (OSTBS) and Quasi Orthogonal codes (QSTBC) [8] for these two configurations, respectively. Vertical Bell Laboratories Space-Time (VBLAST) [9] will also be studied. Secondly, the performances of these algorithms will be explained from the MIMO channel characteristics deduced from measurement campaigns and from the theoretical modeling of the propagation based on the modal theory. The frequency band under consideration is around 3 GHz.

After a brief presentation of the site of measurements and of the theoretical propagation model, path loss and fading distribution are presented in Section II. In Section III, MIMO related characteristics as correlation between array elements and condition number of the transfer matrices are studied as a function of the distance between Tx and Rx. Performances of MIMO algorithms are detailed in Section IV and explained from the channel characteristics.

II. Propagation Characteristics

A. Geometry of the Tunnel and Measurement Procedure

Measurements have been carried out in a straight arched empty tunnel, 3 km long. Its transverse section was semicircular and the diameter of the cylindrical part was 8.6 m. The maximum height was 6.1 m at the center of the tunnel. Wideband biconical antennas were connected to the two ports of a vectorial network analyzer (VNA), the frequency range extending from 2.8 GHz up to 5 GHz, the frequency step being 1.37 MHz. However, in this paper, we will focus on narrow band MIMO channels around a center frequency of 3 GHz, but similar results were obtained around 4 and 5 GHz.
Each transmitting (Tx) and receiving (Rx) antenna can be moved on a rail, situated at a height of 1 m above ground owing to a mechanical system controlled by a stepper motor. These rails were placed perpendicular to the tunnel axis and both Tx and Rx antennas were moved with a spatial step of 3 cm along a distance of 33 cm, as shown in Fig. 1, leading to

C. Sanchis-Borras is with the Department of Telecommunications, University San Antonio from Murcia, Guadalupe, 30107, Murcia, Spain (e-mail: csanchispdi.ucam.edu).

J. M. Molina-Garcia-Pardo is with the Information Technologies and Communications Department, Technical University of Cartagena, Cartagena 30202, Spain (e -mail: josemaria.molina@upct.es).

P. Degauque and M. Lienard are IEMN/TELICE, Electronics Deaprtment, University of Lille, 59655 Villeneuve d'Ascq, France, (e-mail: pierre.degauque;martine.lienard@univ-lille1.fr).

This work was carried out in the frame of the CISIT project, France, and also supported by the Ministerio de Educacion y Ciencia, Spain (TEC2010-20841-C04-03).

12 successive positions in the transverse plane. It will thus be possible to analyze the MIMO channel characteristics based on virtual Tx and Rx arrays. The maximum distance of 33 cm was chosen to be in accordance with implementation constraints of an array on the roof of a vehicle.

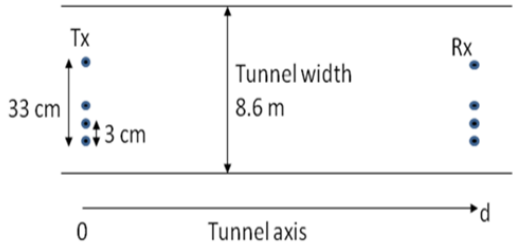

Fig. 1 Configuration of the virtual Tx/Rx arrays inside the tunnel

Along the tunnel axis, the distance between Tx and Rx varied from 50 m up to 500 m. The rail supporting the Rx antenna was thus moved with a step equal to 4 m when 50 m < d < 206 m, and to 6 m when 206 m < d < 498 m. To avoid a prohibitive attenuation in the cables connecting the antennas and the network analyzer, the signal of the Tx port was converted into an optical signal sent through fiber optics. It was then converted back to radio-frequency and amplified, the output power being 1 W. The calibration procedure of the VNA took all these optical and electronic components into account. The channel was stationary since the tunnel was closed to traffic during all the measurements. More details on the procedure of the experiments can be found in [10].

B. Principle of the Theoretical Modeling

The propagation along straight tunnels have been studied for many years, the pioneer works being those described by Mahmoud and Wait [11], among others. It must be emphasized that analytical solutions were obtained for circular or rectangular tunnels since the tunnel cross section corresponds to a line of constant coordinate in an adequate coordinate system. To take the possible complicated shape of the tunnel into account, numerical models have been developed but the description of such models is out of the scope of this paper. Indeed, for physically interpreting the performances of MIMO algorithms, as we will do in Section IV, an analytical model is needed. In previous papers, we have shown from the ray theory, that the propagation in such a semi arched tunnel can be adequately predicted by considering an equivalent rectangular tunnel, For our geometrical configuration, this leads to a rectangular tunnel 8 m wide and 5.6 m high, the walls having an equivalent conductivity and permittivity equal to 10^{-2} S/m and 5, respectively [12].

Another and more suited approach for our application is to use the modal theory, since the tunnel behaves as a lossy oversized waveguide supporting EH_{mn} hybrid modes of order (m,n). If the cross section of the tunnel is in the (x, y) plane, the electric field at any point (x, y, z) can be expressed as:

$$E(x,y,z) = \sum_m \sum_n \alpha_{m,n}(z)\, e_{m,n}(x,y) \qquad (1)$$

where $e_{m,n}(x,y)$ is the normalized modal eigenfunction and $\alpha_{m,n}(z)$ is the modal coefficient at any cross-sectional plane, and thus corresponds to the weight of the mode at the axial distance z. This modal coefficient is defined by:

$$\alpha_{m,n}(z) = \beta_{m,n} e^{-jk_{m,n}z} \qquad (2)$$

In this formula, $k_{m,n}$ is the propagation constant and $\beta_{m,n}$ is the complex amplitude of the mode in the excitation plane. The analytical expressions of the modal eigenfunction and of the propagation constant in terms of the geometrical and electrical characteristics of the tunnel can be found in [6].

To conclude this brief overview of the modal approach, let us mention that the attenuation of a mode along the z axis increases with the order (m, n) of this mode.

C. Path loss and Fading Distribution

In a first step, it is interesting to extract information on the mean path loss. Curves in Fig. 2 represent its variation versus the distance between Tx and Rx. The received signal at 50 m was chosen as a reference.

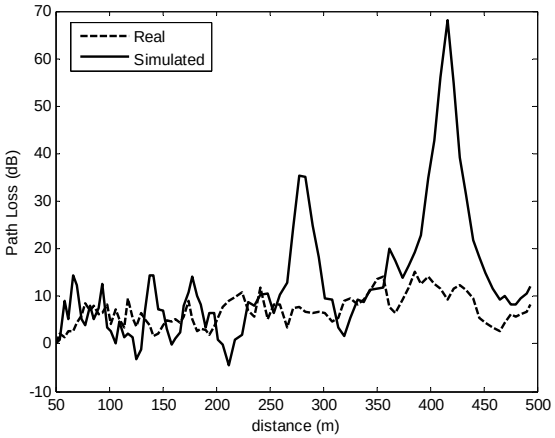

Fig. 2 Average path loss around 3 GHz. Comparison between the values deduced either from measurements (dotted line "real") or from the theoretical modeling (continuous line "simulated")

The experimental curve (dotted line) has been deduced from the measurement of the S_{12} parameter and averaged over the 144 possible combinations of Tx and Rx in the successive transverse planes (see Fig. 1) and over few frequencies in a frequency band smaller than the channel coherence bandwidth. In this example, the coherence bandwidth being larger than 50 MHz, the averaging was thus made on 15 frequency points, corresponding to a band of 25 MHz around 3 GHz. The continuous line in Fig. 2 corresponds to the theoretical curve deduced from the analytical model based on the modal theory. We see that the mean path loss between 50 m and 500 m does not exceed 10 dB, due to the guiding effect of the tunnel. The theoretical curve exhibits a strong attenuation at 280 m and at 420 m due to a destructive interference between the first order modes which are the less attenuated ones. However, such a local variation is not experimentally observed, this discrepancy being probably due to the difference in shape of the tunnel cross section.

In a second step, the Cumulative Distribution Function (cdf) of the received signal has been calculated in various zones of the tunnel. An example is given in Fig. 3 for the zone situated near Tx, i.e. between 50 m and 150 m. The curves in Fig. 3 have been deduced from the path loss calculated or measured on the 144 possible combinations of Tx and Rx , for 25 successive axial distances between 50 m and 150 m and for 15 frequencies as mentioned in the previous paragraph. As a comparison, the Rayleigh distribution has also been plotted. To make easier the comparison between these curves, all the median values were normalized to 0 dB.

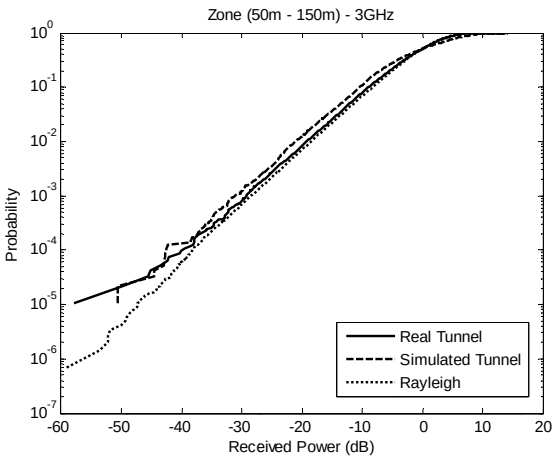

Fig. 3 Cumulative distribution function of the field amplitude "near" the transmitter (between 50 m and 150 m) and deduced either from measurements or from the theoretical modeling. Curve corresponding to a Rayleigh distribution has also been plotted

We see that even with a small spread of the angles of departure/arrival of the rays, the cdf of the received signal follows a Rayleigh distribution. Furthermore, other curves plotted in a zone far from Tx, between 400 m and 500 m, show that the probability to get important fading is less important than near Tx. These results can be easily explained from the modal theory. Indeed, let us define the "active modes" at a distance *z* from Tx, as the modes whose relative amplitudes, normalized to the amplitude of the strongest mode, are greater than a given threshold, chosen in the following example to -6 dB. Table I gives this number of active modes deduced from the theoretical model and for different values of *z*.

TABLE I
NUMBER OF ACTIVE MODES AT VARIOUS DISTANCES Z FROM TX.

Distance Tx-Rx	50 m	150 m	300 m	500 m
Number of active modes	70	32	22	18

Spatial fluctuations of the amplitude of the Rx signal being due to the interference between modes, fading distribution will tend to a Rayleigh distribution if the number of active modes is very important, as it occurs near Tx. On the contrary, at large distances, high order modes suffer significant attenuation and the number of active mode strongly decreases.

III. CHARACTERIZATION OF THE MIMO CHANNELS

In the following, we will study 2 MIMO configurations, denoted MIMO (2,2) and MIMO (4,4), the number of Tx/Rx array elements being equal to 2 or to 4, respectively. In both cases, the maximum length of the array is 27 cm (Fig. 4). The $\boldsymbol{H}$ matrices are immediately deduced from the measurements made for all positions of the Tx/Rx antenna, as shown in Fig. 1.

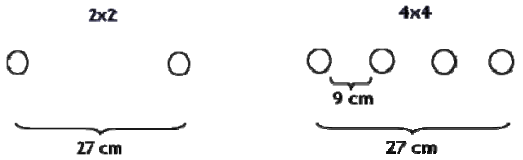

Fig. 4 Configuration of the antenna array for MIMO (2,2) and MIMO (4,4)

Since measurements have been made in the transverse plane by moving an antenna with a step of 3 cm and on a maximum of 33 cm, 9 MIMO channels can be extracted from measurements for a given axial distance *z* between Tx and Rx. The variation, deduced from the measurements of the $\boldsymbol{H}$ matrices, of the mean correlation coefficient ρ_{tx} between 2 Tx array elements, either 9 cm or 27 cm apart, is plotted in Fig. 5.

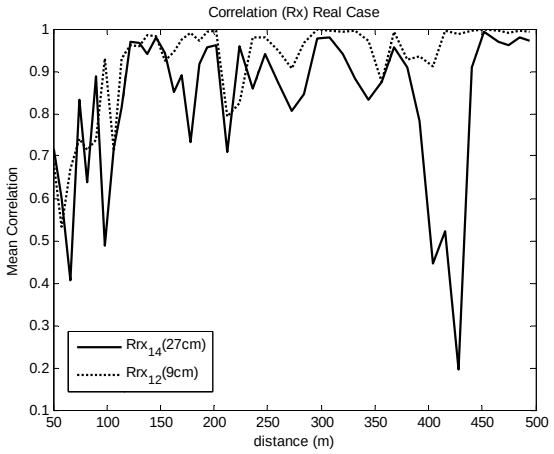

Fig. 5 Mean correlation between two array Tx elements, either 9 cm or 27 cm apart.

Near the Tx, the correlation for array elements 9 or 27 cm apart, is on the order of 0.7. However, when Rx moves away from Rx, ρ_{tx} rapidly increases to reach 0.9 for distances greater than 150 m. This is due to the decrease of the number of active modes, as outlined in the previous section (cf. Table I). Similar results were obtained for the correlation between the Rx array elements.

The performances of MIMO systems may also depend on the condition number *CN* of the *H* matrix, defined as the ratio of its largest eigenvalue to its smallest eigenvalue. Curves in Fig. 6 show the variation of *CN* both for MIMO (2,2) and MIMO (4,4) configurations and deduced either from the experiments or from the theoretical modelling.

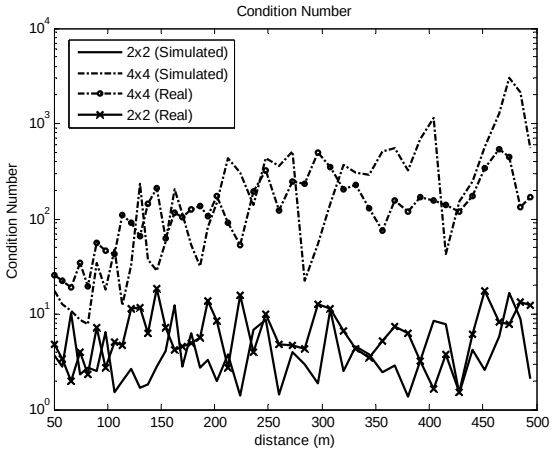

Fig. 6 Variation of the condition number of the ***H*** transfer matrix for a MIMO (2,2) or for a MIMO (4,4) configuration. The dotted lines and the continuous lines refer to values deduced from measurements or from the theoretical modelling, respectively

We first note the good agreement between predicted and experimental values. For MIMO (2,2), there is only a very slight increase of *CN* with distance, its mean value being 8. On the contrary, for MIMO (4,4), *CN* reaches important values, greater than 100 for $z > 130$ m. As for the correlation, this variation of *CN* is due to the decrease of active modes.

IV. Performances of Few MIMO Algorithms

The channel capacity of a narrow band MIMO (*M*, *N*) system, where *M* and *N* are the number of transmitting and receiving antennas, and for a channel realization ***H***, is given by [1], [2]:

$$C = \log_2\left(\det\left|\boldsymbol{I}_N + \frac{SNR}{M}\boldsymbol{H}\boldsymbol{H}^H\right|\right) \quad (3)$$

where $\boldsymbol{I}_N$ is the *N*x*N* identity matrix, $(\ )^H$ is the transpose conjugate operation and *SNR* is the signal-to-noise ratio at the receiver. In a tunnel, despite the fact that the spread of the angle of departure and of the angle of arrival of the rays are small, on the order or less than 10° for a distance Tx-Rx larger than 50 m [13], it has been shown that MIMO strongly improves the capacity, owing to the modal diversity [6]. Indeed, if for example we assume a *SNR* of 15 dB, and by introducing ***H*** measured matrices in (3), the capacity of a MIMO (4, 4) system will be 16 bits/s/Hz at a distance of 50 m from Tx but decreases to 13 bits/s/Hz at 500 m, due to the decrease of the number of active modes. However, the capacity remains higher than for the SISO (Single Input Single Output) case equal to 5 bits/s/Hz in a Rayleigh environment.

If the comparison of channel capacity between MIMO and SISO is interesting to outline the improvement obtained with MIMO, it is however needed to check the robustness of MIMO algorithms for a communication link in a tunnel environment, due to the important correlation between array elements and of the increase with distance of the condition number of the ***H*** matrix.

To achieve this goal, we choose as a reference configuration, a SISO transmission with a 16 QAM (Quadrature Amplitude Modulation). To make a fair comparison with MIMO, the modulation scheme is chosen in such a way that the bit rate is the same whatever the configuration, SISO or MIMO. Furthermore 2 MIMO algorithms were considered: VBLAST and OSTBC or QSTBC codes. The symbol detection method is based on the Minimum Mean Squared Error (MMSE) algorithm. The modulation for each configuration is summarized in Table II.

TABLE II
Modulation Scheme for the Different MIMO and SISO Configurations

Configuration	Modulation
SISO	16QAM
2x2 MIMO-VBLAST	QPSK
4x4 MIMO-VBLAST	BPSK
2x2 MIMO-OSTBC	16QAM
4x4 MIMO- QSTBC	16QAM

A software tool was developed for simulating the communication link (Matlab based), the input in this tool being either measured or theoretical ***H*** matrices. The bit error rate (BER) was deduced from the estimated symbols, the number of transmitted symbol for each channel realization being of 10^5. This leads to a minimum detectable BER of 10^{-5}. We assume that the *SNR* is constant whatever the position of the Rx antennas in the tunnel and equal to 10 dB. Curves in Fig. 7 give the BER obtained by using the VBLAST algorithm.

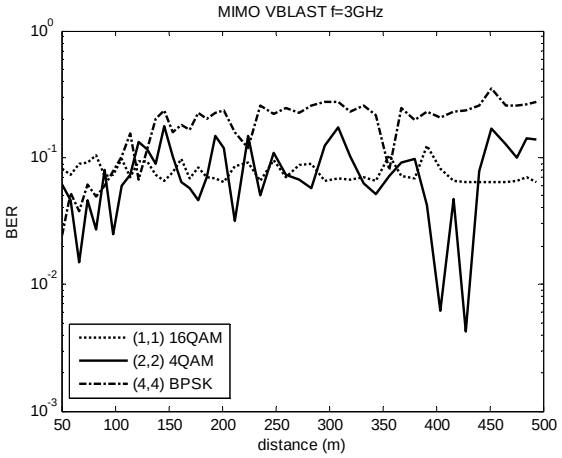

Fig. 7 Bit error rate along the tunnel with SISO, MIMO (2,2) and MIMO (4,4) and using the VBLAST scheme. The SNR is of 10 dB

Near Tx, up to about 100 m, the comparison of the 3 curves shows that the BER is slightly improved with MIMO. Beyond this distance, MIMO (2,2) and SISO gives nearly the same results but MIMO (4,4) presents the worst performances. This

is the consequence of the correlation between array elements which strongly increases (Fig. 5), the condition number of the ***H*** matrices being nearly constant for MIMO (2,2) but becoming greater than 100 if z > 130m (Fig. 6). The theoretical curves deduced from ***H*** calculated with the modal theory have the same behavior but are not put in Fig. 7 for clarity reason.

If now OSTBC, with MIMO (2,2), and QSTBC, with MIMO (4,4), are used, Fig. 8 shows that the average BER does not depend on distance and, contrary to what happens with VBLAST, the BER decreases if the number of array elements increases for 2 to 4. In all cases, MIMO outperforms SISO.

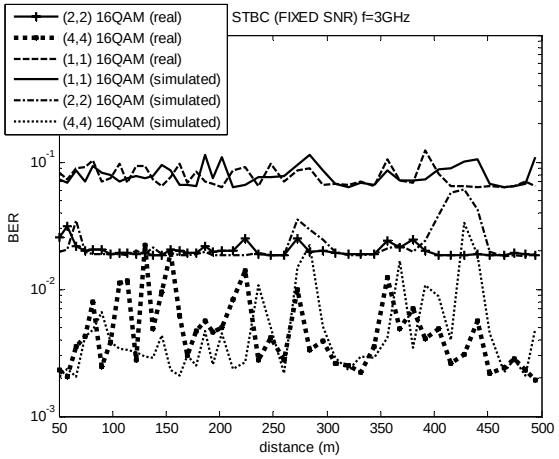

Fig. 8 Same as in Fig. 7 but with the OSTBC scheme for MIMO (2,2) and QSTBC for MIMO (4,4). Curves have been plotted using either measured or theoretical ***H*** matrices

V. Conclusion

The MIMO channel characteristics around 3 GHz deduced either form the modal theory or from measurements strongly varies with the distance between the transmitter and the receiver. As soon as this distance becomes greater than 100 m, the VBLAST algorithm does not give satisfying results due to the increase of the correlation between array elements and of the condition number of the transfer matrix. OSTBC or QSTBC must thus be chosen and, for the same bit rate, outperforms SISO in terms of bit error rate. Similar results were obtained for other carrier frequencies between 3 and 5 GHz.

References

[1] G.J. Foschini and M.J. Gans, "On limits of wireless communication in a fading environment when using multiple antennas", *Wireless Personal Commun*, vol 6, no. 3, pp. 311 – 335, 1998.

[2] I.E. Telatar, "Capacity of multi-antenna Gaussian channel", *European Trans. on Telecom.*, vol. 10, no. 6, pp. 585-595, 1999

[3] M. Lienard, P. Degauque, J. Baudet, and D. Degardin, "Investigation on MIMO channels in subway tunnels," *IEEE J. on Selected Areas in Commun.*, vol. 21, no. 3, pp. 332–339, 2003.

[4] J. Alonso, B. Izquierdo, S. Capdevila, and J. Romeu, "Preliminar propagation and MIMO experiments in train tunnels at 5.8 GHz," in *Conf. Proc. IEEE Int. Symp. On Antennas and Propag.*, pp. &-4, 2009.

[5] S. Loyka, "Multiantenna capacities of waveguide and cavity channels", *IEEE Trans. Vehicular Technology*, vol. 54, pp. 863–872, 2005.

[6] J.-M. Molina-Garcia-Pardo, M Liénard, P. Degauque, D. Dudley and L. Juan Llácer, "Interpretation of MIMO Channel Characteristics in Rectangular Tunnels from Modal Theory", *IEEE Trans. on Vehicular Techno.*, vol. 57, no. 3, pp. 1974-1979, April 2008.

[7] C. Sanchis-Borras, J.-M. Molina-Garcia-Pardo, M Lienard, P. Degauque and L. Juan Llacer, "Performance of QSTBC and VBLAST algorithms for MIMO channels in tunnels", *IEEE Antennas and Propag. Letters*, vol. 9, pp. 906-909, 2010.

[8] C. F. Mecklenbrauker and M. Rupp, "Generalized Alamouti codes for trading quality of service against data rate in MIMO UMTS," EURASIP Journal on Applied Signal Processing, vol. 2004, no. 5, pp. 662–675, 2004.

[9] P.W. Wolniansky, G. J. Foschini, G.D. Golden and R.A. Valenzuela, "V-BLAST: An architecture for realizing very high data rates over the rich-scattering wireless channel," in *Proc. URSI Symposium*, pp. 295-300, September 1998.

[10] Molina-Garcia-Pardo, J. M., M. Lienard, and P. Degauque, "Propagation in tunnels: Experimental investigations and channel modeling in a wide frequency band for MIMO applications," *EURASIP J. Wirel. Commun. and Networking*, Article ID 560571, doi:10.1155/2009/560571, 2009

[11] S.F. Mahmoud and J.R. Wait, "Geometrical optical approach for electromagnetic wave propagation in rectangular mine tunnels", *Radio Sci.*, vol. 9, pp. 1147 – 1158, 1974.

[12] Molina-Garcia-Pardo, J. M., M. Lienard, A. Nasr, and P. Degauque, "On the possibility of interpreting field variations and polarization in arched tunnels using a model for propagation in rectangular or circular tunnels," *IEEE Trans. Antennas Propag.*, vol. 56, no.4, pp. 1206-1211, 2008.